

Optical nonlinearity and existence conditions for quasi-steady-state photorefractive solitons

Eugenio DelRe

Laboratorio di Ottica e Fotonica, Dipartimento di Ingegneria Elettrica e dell'Informazione, Università dell'Aquila, 67040 Monteluco di Roio, L'Aquila, Italy and Centro Ricerca e Sviluppo SOFT, Istituto Nazionale della Materia—Consiglio Nazionale della Ricerche 00185 Roma, Italy

Elia Palange

Laboratorio di Ottica e Fotonica, Dipartimento di Ingegneria Elettrica e dell'Informazione, Università dell'Aquila, 67040 Monteluco di Roio, L'Aquila, Italy and Laboratorio Regionale SENSOR-CASTI, Istituto Nazionale della Materia—Consiglio Nazionale della Ricerche 00185 Roma, Italy

Received April 24, 2006; revised July 14, 2006; accepted July 20, 2006; posted July 25, 2006 (Doc. ID 70066)

Generalizing soliton description using spatiotemporal wave variables, we identify and experimentally validate the nonlinearity supporting quasi-steady-state solitons in biased photorefractive crystals for the one-dimensional case, the transient counterpart of the explicit one-dimensional screening soliton theory. The approach leads to a non-Kerr-like spatially local exponential nonlinearity and explicitly provides soliton existence conditions. These find quantitative agreement with a series of experiments in potassium lithium tantalate niobate and reproduce previously described transient behavior. © 2006 Optical Society of America

OCIS codes: 190.5330, 190.5530.

1. INTRODUCTION

Photorefractive quasi-steady-state (QSS) solitons are observed both as one-plus-one-dimensional (1+1D) slabs and as 2+1D needles, in various crystal types and phases, as bright and dark, single-component, and incoherent solitons.^{1–13} They form the building block of soliton electroactivation,¹⁴ an important expansion to the variety of established soliton applications.^{15,16} This is because, in distinction to steady-state (SS) screening solitons,^{17–19} QSS solitons do not require the homogeneous illumination of the entire crystal to form²⁰ but allow the sequential imprinting of single-soliton waveguides in different portions of the sample without erasing previously written ones. This has spurred renewed interest in the effect, whose study and phenomenological characterization have developed in the past decade.^{1–11,13} One important still-open issue is the identification of the effective optical nonlinearity that leads, during the transient, to the QSS self-trapping.^{1,3,5,6}

Phenomenologically, a QSS soliton,²¹ in the basic 1+1D case, is characterized by the following properties (similar statements transfer to the 2+1D case).

(I) For an initially homogeneous biased material, the initially diffracting light beam undergoes a cycle during which it first progressively self-focuses; after a transient t_c , settles into a self-trapped wave; undergoes a decelerated evolution for a temporal window t_p , the soliton plateau, during which the actual transverse beam intensity full width at half-maximum (FWHM) Δx changes slightly, but the balancing of self-focusing and diffraction along the propagation axis z is approximately maintained; and,

finally, for $t > (t_c + t_p)$, decays into a distorted and once again diffracting beam, ending the cycle.

(II) The cycle occurs for a range of different experimental conditions, i.e., of input beam launch Δx_0 ; value of applied external field E_0 , which must be larger than the diffusion and charge-displacement fields; and of beam peak intensity I_p , which must be much larger than the natural or artificial background illumination I_b .

(III) The minimum beam size, in normalized soliton units, which approximates the beam size during the plateau, has a characteristic value (see, for example, Ref. 8), implying that the observed minimum beam size Δx_{\min} is intensity independent and decreases as E_0 increases, all else left unaltered, a dependence that tends to weaken for wide beams.

(IV) All the time scales, i.e., t_c and t_p , are inversely proportional to I_p , and if $\Delta x_0 \approx \Delta x_{\min}$, $t_p \gg t_c$.

(V) In conditions in which both the QSS and the generally different (wider and less intense) SS soliton can form, the full cycle precedes in time the formation of the SS soliton (see, for example, Refs. 7–9).

(VI) The cycle occurs both for monochromatic and for white light.

In this paper we develop, for what we believe to be the first time, a theory for 1+1D QSS solitons, compatible with these phenomenological statements. The finding hinges on the formulation of a generalized soliton propagation equation that makes use of a single spatiotemporal wave variable. Our specific goal is to explicitly predict and experimentally validate the underlying nonlinearity and the resulting soliton-width-nonlinearity relationship [i.e.,

property (III)], providing a means to predict soliton parameters in a fashion that emulates the screening nonlinearity for 1+1D SS solitons.

2. MOTIVATION

At present, the understanding of QSS phenomenology is based on mutual phase modulation induced by a superposition of multiple two-wave-mixing processes.^{1,3,5,6} This leads to a spatially nonlocal nonlinearity. The theory is time independent [in contrast to properties (I) and (IV)] and does not provide a method to predict the behavior of statement (III). Refining the picture through the introduction of a soliton threshold^{3,5} leads to an overestimated value of required E_0 (for example, see results in Refs. 2 and 4). More radically, the theory is based on wave mixing, a coherence-driven effect that cannot be reconciled with property (VI). More elaborate time-dependent approaches based on numerical simulation, although not providing an explicit and controllable picture, have identified most of the phenomenological traits, this underlining that the effect must arise from the basic time-dependent photorefractive model.⁷⁻⁹ For example, an in-depth investigation of the predicted and observed phenomenology well summarized in Ref. 8 allowed the formulation of statement (III), in particular, finding that in normalized soliton units the soliton FWHM has a minimum at approximately 3, but, as stated therein, no reason for this important characteristic was found. The difficult situation is well depicted by the failure of a direct analogy with the screening model, in the limit of low I_b , implied by statement (V).

3. MODEL AND SELF-CONSISTENT APPROACH

Photorefractive self-action is mediated by the formation of a light-driven spatially resolved electric field E that changes beam evolution by electro-optically modifying the local index of refraction $n = n_b + \Delta n(E)$. In the 1+1D band-transport model, the x -directed field $E(x, z, t)$ obeys the cumulative equation $\partial_\tau Y + QY = 1$, or

$$Y = \exp\left(-\int_0^\tau Q d\tau'\right) \left[1 + \int_0^\tau d\tau' \exp\left(\int_0^{\tau'} Q d\tau''\right)\right], \quad (1)$$

for conditions in which displacement charge, diffusion, and photovoltaic effects can be neglected, i.e., in the regime of experiments [property (II)].²² In Eq. (1), $\tau = t/t_d$, $t_d = \epsilon_0 \epsilon_r \gamma N_a / [q \mu s (N_d - N_a) I_b]$ is the so-called dielectric relaxation time, γ is the charge recombination rate, N_a is the density of acceptor impurities, N_d is that of donors, q is the electron charge, μ is the electron mobility, s is the donor impurity photoionization efficiency, I_b is the equivalent background illumination, $Y = E/E_0$, and $Q = (1 + I/I_b)$, I being the beam intensity. Equation (1) involves a spatially resolved time nonlocality or memory that at SS, i.e., for $\tau \gg 1$, leads to the screening soliton expression $Y = 1/Q$, or $E = E_0/(1 + I/I_b)$.

According to properties (I) for $\tau_c < \tau < \tau_p$ the normalized beam intensity Q becomes approximately time independent and factors out of the integrals. Furthermore, be-

cause of property (IV), even the more complicated contribution to the integral associated with the memory of the initial transient phase (where Q is inherently time dependent) can be neglected. The result is that Eq. (1) can be approximated by

$$Y \approx \exp(-Q\tau) + 1/Q - (1/Q)\exp(-Q\tau) \rightarrow Y \approx \exp(-Q\tau), \quad (2)$$

the second form being valid because of property (II) ($Q \gg 1$). This is true except for the very tails of the beam shape, and for time scales involved τ such that $\tau \ll \ln Q/Q$, a condition whose validity is discussed below.

To formulate the basic nonlinear propagation equation, we note that the slowly varying part of the optical field A [i.e., $I(x, z, t) = |A|^2$] obeys the parabolic wave equation

$$[\partial_z + (i/2k)\partial_{xx}]A = -(ik/n_b)\Delta n A, \quad (3)$$

where k is the wave vector of the monochromatic light beam and Δn is the nonlinear index modulation, the result of the electro-optic response to the electric field described by expression (2). The electro-optic response depends both on crystal parameters and beam geometry and on the actual phase of the sample. For ferroelectrics, such as strontium barium niobate and potassium niobate, $\Delta n = -(1/2)n_b^3 r_{\text{eff}} E$, r_{eff} being the effective linear electro-optic coefficient. Defining $\Delta n_0 = -(1/2)n_b^3 r_{\text{eff}} E_0$, expression (2) implies that $\Delta n = \Delta n_0 Y = \Delta n_0 \exp(-Q\tau)$. For paraelectrics, such as room-temperature potassium lithium tantalate niobate (KLTN), the electro-optic response is quadratic in the electric field, $\Delta n = -(1/2)n_b^3 g_{\text{eff}} \epsilon_0^2 \epsilon_r^2 E^2$, where g_{eff} is the effective quadratic electro-optic effect, and expression (2) implies $\Delta n = \Delta n_0 (Y)^2 = \Delta n_0 \exp(-2Q\tau)$, where $\Delta n_0 = -(1/2)n_b^3 g_{\text{eff}} \epsilon_0^2 \epsilon_r^2 E_0^2$. For both cases the single form

$$\Delta n = \Delta n_0 \exp(-mQ\tau) \quad (4)$$

holds, with $m = 1(2)$ for ferroelectrics (paraelectrics). Note that, in these terms, time enters into Eq. (3) through Eq. (4) and acts as a parameter (for example, see Ref. 22). Finally, to self-consistently reduce our analysis to cases leading to solitons, we impose a z -invariant intensity condition by taking $A(x, z) = u(x) \exp(i\Gamma z) (I_b)^{1/2}$, Γ being the soliton propagation constant. With this condition, inserting Eq. (4) into Eq. (3), we obtain the nonlinear equation

$$[\Gamma u + (1/2k)\partial_{xx}u] = -(k/n_b)\Delta n_0 \exp(-mu^2\tau)u, \quad (5)$$

where once again the property (II) has been used to approximate $Q \approx I/I_b$. To further cast the equation into a form suitable to the identification of the soliton waveforms and their existence conditions, we generalize previous self-consistent approaches by changing the wave variable from $u(x)$ to $w(\xi) = (m\tau)^{1/2} \tilde{u}(\xi)$, where $\xi = x/d$ is the transverse coordinate normalized to the nonlinear length $d = (-2kb)^{-1/2}$ and $b = (k/n_b)\Delta n_0$. The result is

$$d^2 w(\xi)/d\xi^2 = -[\gamma - \exp(-w^2)]w(\xi), \quad (6)$$

where $\gamma = \Gamma n_b / (\Delta n_0 k)$ is the normalized propagation constant. Since no first-derivative terms appear, we can explicitly relate γ to experimentally relevant parameters. Equation (6) can be integrated once through quadrature, leading to the algebraic relationship

$$p^2 - p_0^2 = -\gamma w^2 + \gamma w_0^2 - \exp(-w^2) + \exp(-w_0^2), \quad (7)$$

where $p = dw/d\xi$, $p_0 = (dw/d\xi)_{\xi=0}$, $w_0 = w(\xi=0) = u(\xi=0)(m\tau)^{1/2} = u_0(m\tau)^{1/2}$. To predict bright solitons, we must require that $(d\tilde{u}/d\xi)_{\xi=0} = 0$, i.e., $p_0 = 0$, and that $\tilde{u}(\xi) \rightarrow 0$ and $d\tilde{u}/d\xi \rightarrow 0$ for $\xi \rightarrow \infty$, which implies that $w(\xi) \rightarrow 0$ and $dw/d\xi \rightarrow 0$ for $\xi \rightarrow \infty$ for any finite value of τ (and even for $\tau \rightarrow \infty$ for a polynomial or exponential tail shape). This leads to $\gamma = [1 - \exp(-w_0^2)]w_0^{-2}$ and the soliton profile equation

$$d^2w(\xi)/d\xi^2 = -\{[1 - \exp(-w_0^2)]w_0^{-2} - \exp(-w^2)\}w(\xi), \quad (8)$$

characterized by a spatially local²³ exponential nonlinearity, in distinction to other known soliton families. The same procedure can be extended to dark self-trapping conditions.^{11,12,20} The procedure leads to the set of soliton existence conditions that form a generalized existence curve in the wave peak amplitude $w_0 = u(\xi=0)(m\tau)^{1/2} = u_0(m\tau)^{1/2}$ and the $\Delta\xi$ (i.e., the normalized soliton intensity FWHM $\Delta\xi = \Delta x/d$) parameter plane, as shown in Fig. 1. Equation (3) with Eq. (4) is a generalized nonlinear Schrödinger equation, and the stability of the solitons of Eq. (8) can be established through an approximate but explicit evaluation of the soliton power P as a function of the propagation constant Γ and subsequent application of the Vakhitov–Kolokolov criterion (i.e., $\partial P/\partial \Gamma > 0$).²⁴ Since only the waveforms that have an approximately constant width are of interest here, although the actual profiles are not explicitly available, the assumption $P \propto w_0^2$ is approximately valid, and, with $\gamma = \Gamma n_0 / (\Delta n_0 k) = [1 - \exp(-w_0^2)]w_0^{-2}$, the condition for the inverse function $\partial \Gamma/\partial P > 0$ is satisfied for all values of P ($P > 0$ and $\Delta n_0 < 0$).

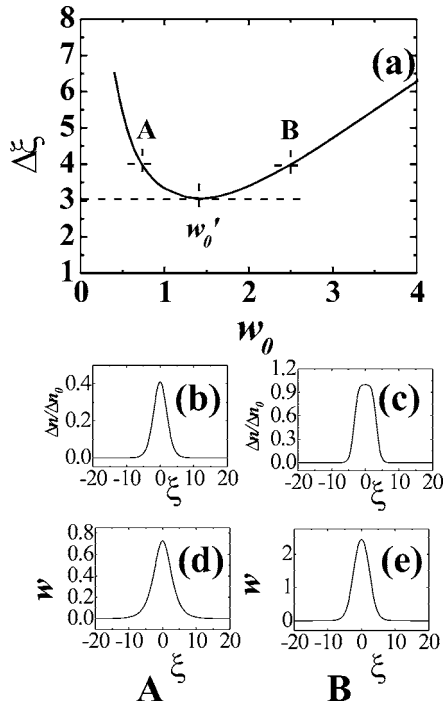


Fig. 1. (a) Existence curve for bright solitons of Eq. (8); (b), (c) index patterns and (d), (e) soliton profiles for the two points A and B, respectively, before and after the onset of strong saturation, highlighting the reshaping of the beam tails [(d) and (e)].

4. SOLITON EXISTENCE CONDITIONS

The results described in Fig. 1 [and Eq. (8) itself] confer a picture now analogous to other soliton-supporting mechanisms (see, for example, Refs. 17–19). However, whereas Eq. (8) describes the entire family of solitons for any value of w_0 , its relevance to QSS photorefractive solitons is self-consistently limited to those conditions [a product of (I)–(VI)] that allow the passage from Eq. (1) to expression (2). In particular, the waveform u must be approximately independent of time, which means that the parameters of interest must be those for which the beam shape changes little as w_0 (i.e., τ) increases. This occurs in proximity to the reshaping region identified by the minimum at w_0' [see Fig. 1(a)] corresponding to the onset of strong saturation in the nonlinearity [see the comparison of condition A to condition B, w_0' being intermediate, in Figs. 1(b)–1(e)], which also indicates a maximum value of nonlinear self-action. This means that, during the cycle of statement (I), we expect the minimum value of Δx_{\min} to correspond to the minimum value $\Delta\xi_{\min} = \Delta\xi(w_0')$. This allows the direct prediction of Δx_{\min} as a function of E_0 , i.e., of property (III). From Eq. (8) this existence relationship is

$$\Delta x_{\min} = \frac{\Delta\xi_{\min}\lambda}{2\pi n_0^2 a_m} E_0^{-m/2}, \quad (9)$$

where from Fig. 1(a), $\Delta\xi_{\min} = 3.07$, $a_1 = (r_{\text{eff}})^{1/2}$, and $a_2 = \epsilon_0 \epsilon_r (g_{\text{eff}})^{1/2}$. The condition at the basis of the approximate expression of relation (2) can now be more precisely quantified. It implies that for the cycle of property (I) the role of the screening term $1/Q$ is negligible for the diffraction–self-focusing interplay [a situation that fits well with property (V)]. This translates to $\Delta x_s \gg \Delta x_{\min}$, Δx_s being the screening soliton size for the given E_0 and u_0 .^{17–19} Through soliton asymptotics²⁵ and Eq. (9), this translates into the general (i.e., dimensionless) condition $u_0^2 \gg [\Delta\xi_{\min}/(\pi/2)]^2 = 4$ for $m = 1, 2$.

The $m = 1$ prediction is illustrated in Fig. 2(a) and compared with the prediction of the nonlocal wave-mixing theory.^{3,5} For the 1+1D case, lack of published results precludes a quantitative comparison with experiments. As a matter of illustration, the single 1+1D point described in Ref. 4 is compared with the prediction, but this can constitute proof of agreement to theory only through further experiment. More importantly, the prediction provides the explicit value of the minimum normalized soliton width $\Delta\xi_{\min} \approx 3.07$, a value that fully explains previous predictions of statement (III).^{8,9} Furthermore, the result of Eq. (9) is able to describe the qualitative part of proposition (III), by which for large values of Δx_{\min} , self-trapping will occur for similar values of E_0 . From Fig. 2(a), for example, this is particularly evident for $E_0 \sim 0.1$ kV/cm and $\Delta x_{\min} \sim 30$ μm . A specular insensitivity in external bias could be observed for highly confined beams. Finally, again for illustrative purposes, we have also plotted the 2+1D data that are available, but here a comparison requires the elaboration of a 2+1D theory.

5. EXPERIMENTS

We carried out a series of experiments in a $3^{(x)}$ mm \times $2.6^{(y)}$ mm \times $6^{(z)}$ mm sample of photorefractive KLTN.

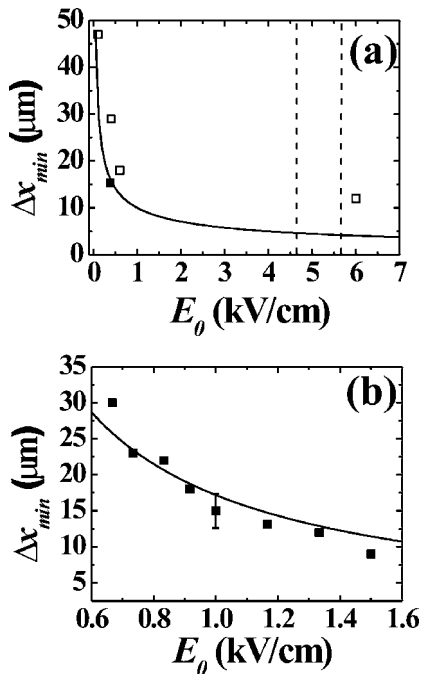


Fig. 2. (a) Predicted self-trapping existence conditions (solid curve) from Eq. (9) for noncentrosymmetric samples ($m=1$) for the parameters of Ref. 4. Dashed lines indicate the region of existence predicted by the nonlocal theory of Ref. 3, and the hyperbolic form of Eq. (9) well reproduces the observed insensitivity of Δx_{\min} on E_0 for large beams (see text). For illustrative purposes, the single 1+1D data point described in Ref. 4 is also plotted (filled squares), along with data for 2+1D solitons (open squares) from Ref. 2 (minimum in the x direction). (b) Self-trapping existence conditions for centrosymmetric samples ($m=2$): experimental results (squares) compared with theory (solid curve).

The crystal is heated through a current-controlled Peltier junction above its ferroelectric phase transition at $T_c \approx 15^\circ\text{C}$ to $T=21^\circ\text{C}$. Here the crystal is paraelectric and manifests a quadratic electro-optic effect, so the transient self-trapping occurs in the $m=2$ case. The measured crystal parameters are $n_b \approx 2.35$, $g_{\text{eff}} \approx 0.12 \text{ m}^4\text{C}^{-2}$, and $\varepsilon_r \approx 8.4 \times 10^3$. A cw argon-ion laser ($\lambda=514 \text{ nm}$) was used in part to achieve the y -polarized (low) background illumination (I_b) and in part for the soliton beam, which was x polarized parallel to the direction of the external bias field. An approximate 1D launch Gaussian beam with an input Δx_0 varying from 8 to 30 μm (and the FWHM in the vertical y direction fixed to $\Delta y \approx 8 \text{ mm}$) was achieved through the use of different confocal lenses combined with a final cylindrical lens with a 15 cm focal length and an output iris. The intensity distribution at the input and output facets of the sample was imaged onto a CCD camera, which allowed for a continuous monitoring and data acquisition of the beam profile, width, and peak intensity.²⁶

To test the basic prediction of Eq. (9), for each given value of input launch Δx_0 , we detected the output time dynamics of the intensity distribution, characterized by a sequence of a focusing, quasi-stationary, and defocusing stages. By varying the value of applied E_0 , we observed a change in the value of the minimum output Δx_{\min} during the quasi-stationary stage. In Fig. 2(b) we report the values of applied E_0 required to have $\Delta x_{\min} \approx \Delta x_0$, i.e., the formation of a QSS soliton. The soliton beam power was

$P=60 \mu\text{W}$ at input, whereas the input intensity ratio was, for each point, fixed to $u_0^2 \equiv (I_p/I_b) \approx 160$.

The agreement with predictions is evident, validating Eq. (9) and, consequently, the self-consistent procedure leading to Eq. (8). In turn, since results are based on measurements of a minimum (FWHM), sensitivity is limited; this is reflected in the errors in data.

We note that congruently with (II), (III), and (IV) Eq. (9) does not contain u_0 , I_b , or I_p . More radically, Eq. (8), which dictates the salient physical features of the self-trapping process, is invariant for transformations of the type $T_\sigma(t, I) \rightarrow (\sigma t, \sigma^{-1} I)$, I being the intensity of the sole soliton beam (this behavior is not true for screening solitons^{17–19}).

6. CONCLUSION

Concluding, we have elaborated a direct self-consistent description of QSS photorefractive solitons, providing the means to relate experimental parameters to observed self-trapping, for both linear and quadratic electro-optic responses. The finding should provide both the basis for the prediction and the description of the actual soliton dynamics in time (for example, the duration of the soliton plateau); its extension to two-dimensional self-trapping, where, however, anisotropy is expected to play a relevant role; and the formulation of a more general physical picture in which space and time lead to new effects based on their mutual interplay.

ACKNOWLEDGMENTS

Research was funded by the Italian Ministry of Research through the Fondo di Investimento per la Ricerca per la Ricerca di Base (FIRB) initiative. Support from the DEWS Center of Excellence, L'Aquila, is acknowledged.

The corresponding author, Eugenio DelRe, can be reached by e-mail at edelre@ing.univaq.it.

REFERENCES

1. M. Segev, B. Crosignani, A. Yariv, and B. Fischer, "Spatial solitons in photorefractive media," *Phys. Rev. Lett.* **68**, 923–926 (1992).
2. G. Duree, J. Schultz, G. Salamo, M. Segev, A. Yariv, B. Crosignani, P. Di Porto, E. Sharp, and R. Neurgaonkar, "Observation of self-trapping of an optical beam due to the photorefractive effect," *Phys. Rev. Lett.* **71**, 533–536 (1993).
3. B. Crosignani, M. Segev, D. Engin, P. Di Porto, A. Yariv, and G. Salamo, "Self-trapping of optical beams in photorefractive media," *J. Opt. Soc. Am. B* **10**, 446–453 (1993).
4. G. Duree, G. Salamo, M. Segev, A. Yariv, B. Crosignani, P. Di Porto, and E. Sharp, "Dimensionality and size of photorefractive spatial solitons," *Opt. Lett.* **19**, 1195–1197 (1994).
5. D. N. Christodoulides and M. I. Carvalho, "Compression, self-bending, and collapse of Gaussian beams in photorefractive crystals," *Opt. Lett.* **19**, 1714–1716 (1994).
6. M. Segev, B. Crosignani, P. Di Porto, A. Yariv, G. Duree, G. Salamo, and E. Sharp, "Stability of photorefractive spatial solitons," *Opt. Lett.* **19**, 1296–1298 (1994).
7. A. Zozulya and D. Anderson, "Nonstationary self-focusing in photorefractive media," *Opt. Lett.* **20**, 837–839 (1995).
8. N. Fressengeas, D. Wolfersberger, J. Maufroy, and G. Kugel,

- “Build up mechanisms of (1+1)-dimensional photorefractive bright spatial quasi-steady-state and screening solitons,” *Opt. Commun.* **145**, 393–400 (1998).
9. M. Wesner, C. Herden, R. Pankrath, D. Kip, and P. Moretti, “Temporal development of photorefractive solitons up to telecommunication wavelengths in strontium-barium niobate waveguides,” *Phys. Rev. E* **64**, 036613 (2001).
 10. M. Asaro, M. Sheldon, Z. Chen, O. Ostroverkhova, and W. E. Moerner, “Soliton-induced waveguides in an organic photorefractive glass,” *Opt. Lett.* **30**, 519–521 (2005).
 11. G. Duree, M. Morin, G. Salamo, M. Segev, B. Crosignani, P. Di Porto, E. Sharp, and A. Yariv, “Dark photorefractive spatial solitons and photorefractive vortex solitons,” *Phys. Rev. Lett.* **74**, 1978–1981 (1995).
 12. M. Chauvet, “Temporal analysis of open-circuit dark photovoltaic spatial solitons,” *J. Opt. Soc. Am. B* **20**, 2515–2522 (2003).
 13. M. Mitchell and M. Segev, “Self-trapping of incoherent white light,” *Nature* **387**, 880–883 (1997).
 14. E. DelRe, B. Crosignani, E. Palange, and A. J. Agranat, “Electro-optic beam manipulation through photorefractive needles,” *Opt. Lett.* **27**, 2188–2190 (2002).
 15. M. F. Shih, M. Segev, and G. J. Salamo, “Circular waveguides induced by two-dimensional bright steady-state photorefractive spatial screening solitons,” *Opt. Lett.* **21**, 931–933 (1996).
 16. J. Petter, C. Denz, A. Stepken, and F. Kaiser, “Anisotropic waveguides induced by photorefractive (2+1)D solitons,” *J. Opt. Soc. Am. B* **19**, 1145–1149 (2002).
 17. M. Segev, G. C. Valley, B. Crosignani, P. DiPorto, and A. Yariv, “Steady-state spatial screening solitons in photorefractive materials with external applied field,” *Phys. Rev. Lett.* **73**, 3211–3214 (1994).
 18. S. R. Singh and D. N. Christodoulides, “Evolution of spatial optical solitons in biased photorefractive media under steady-state conditions,” *Opt. Commun.* **118**, 569–576 (1995).
 19. M. Segev, M. F. Shih, and G. C. Valley, “Photorefractive screening solitons of high and low intensity,” *J. Opt. Soc. Am. B* **13**, 706–718 (1996).
 20. M. Morin, G. Duree, G. Salamo, and M. Segev, “Waveguides formed by quasi-steady-state photorefractive spatial solitons,” *Opt. Lett.* **20**, 2066–2068 (1995).
 21. Note the particlelike properties even during transients [see, for example, C. Denz, W. Krolikowski, J. Petter, C. Weillnau, T. Tschudi, M. R. Belic, F. Kaiser, and A. Stepken, “Dynamics of formation and interaction of photorefractive screening solitons,” *Phys. Rev. E* **60**, 6222–6225 (1999)].
 22. C. Dari-Salisburgo, E. DelRe, and E. Palange, “Molding and stretched evolution of optical solitons in cumulative nonlinearities,” *Phys. Rev. Lett.* **91**, 263903 (2003).
 23. Locality allows extension to incoherent schemes.
 24. See S. Trillo and W. Torruellas, eds., *Spatial Solitons* (Springer, 2001), pp. 211–245.
 25. E. DelRe, A. D’Ercole, and A. J. Agranat, “Emergence of linear wave segments and predictable traits in saturated nonlinear media,” *Opt. Lett.* **28**, 260–262 (2003).
 26. E. DelRe, B. Crosignani, M. Tamburrini, M. Segev, M. Mitchell, E. Refaeli, and A. J. Agranat, “One-dimensional steady-state photorefractive spatial solitons in centrosymmetric paraelectric potassium lithium tantalate niobate,” *Opt. Lett.* **23**, 421–423 (1998).